Title	Modelling and testing of a historic steel suspension footbridge in Ireland
Authors	O'Donnell, Deirdre;Wright, Robert;O'Byrne, Michael;Sadhu, Ayan;Edwards Murphy, Fiona;Cahill, Paul;Kelliher, Denis;Ghosh, Bidisha;Schoefs, Franck;Mathewson, Alan;Popovici, Emanuel M.;Pakrashi, Vikram
Publication date	2017-05-15
Original Citation	O'Donnell, D., Wright, R., O'Byrne, M., Sadhu, A., Edwards Murphy, F., Cahill, P., Kelliher, D., Ghosh, B., Schoefs, F., Mathewson, A., Popovici, E. and Pakrashi, V. (2017) 'Modelling and testing of a historic steel suspension footbridge in Ireland', Proceedings of the ICE - Bridge Engineering, 170(2), pp. 116-132. doi: 10.1680/jbren.15.00047
Type of publication	Conference item
Link to publisher's version	10.1680/jbren.15.00047
Rights	© 2017, ICE Publishing. All rights reserved.
Download date	2024-04-25 10:19:19
Item downloaded from	https://hdl.handle.net/10468/11803

Modelling and Testing of the Landmark Daly's 'Shaky' Bridge

Deirdre O'Donnell,BE; Robert Wright,BE; Michael O'Byrne, BE, PhD; Ayan Sadhu,BE, PhD, M.ASCE; Fiona Edwards Murphy, BE; Paul Cahill,BE, PhD; Denis Kelliher,BE, PhD; Bidisha Ghosh,BE, PhD; Franck Schoefs,BE, PhD; Alan Mathewson,BE, PhD; Emanuel Popovici, PhD, MIEEEand Vikram Pakrashi, BE, PhD, CEng MIEI, M.ASCE

Abstract

Daly's Bridge is a historic steel suspension footbridge in Ireland, known locally as the 'Shaky Bridge' for its noticeable movement under pedestrian loading. While there is concern regarding the performance of the structure, testing or modelling have not been carried out till date and inadequate information exist in relation to carrying out such analyses. In this paper, Daly's bridge is instrumented and tested for the first time and a model of the bridge is established and improved in the process. Apart from ambient vibration, excitation from traversing pedestrians and cyclists is considered. Video analysis of dynamic deflection, a wavelet packet based technique using acceleration responses and dynamic measurements from a cheap smartphone

accelerometer application are used to identify and compare the natural frequency of the bridge. The work contributes to the evidence base of full-scale measurements of instrumenting and analysing responses of aging pedestrian bridges highlighting the complexity, challenges, opportunities and limitations related to varied levels of information available from disparate sources . The study also highlights the need of investigating to what extent cheap sensors can be successfully used as compared to their more expensive and sophisticated counterpart.

ICE Proceedings list of keywords: bridges, field testing and monitoring, maintenance and inspection

1 Introduction

The cost of maintaining and replacing damaged infrastructure worldwide is high, with an estimated $7.6 billion required annually to maintain bridges in the US alone (ASCE, 2013). The need for economically sustainable maintenance of bridges is ever growing as civil infrastructure ages (Catbas et al., 2008; Znidaric et al., 2011), with the instrumentation and testing of such infrastructure becoming more important under such circumstances. In this regard, significant attention has been directed towards pedestrian induced vibrations in footbridges (Leonard, 1966; Nakamura and Kawasaki, 2006; Živanović et al., 2006), with extensive research into the effects and the assessment of pedestrian load conditions being conducted recently (Bruno and Venuti, 2009; Ingólfsson et al., 2012). However, such user induced excitations can also be used to assess the bridge in terms of determining the

dynamic response and modal properties of the structure (Pakrashi et al., 2010; Jaksic et al., 2014; Caetano et al., 2013; Sadhu et al. 2015; Jaksic et al., 2016). The dynamic signature of a bridge is indicative of its serviceability condition and the level of dynamic acceleration can be related to the comfort level to the user (Van Nimmen et al., 2014). Many footbridges are slender structures and have natural frequencies that lie in the domain of dominant harmonics of walking pedestrians (Živanović et al., 2005; Huang et al., 2005).

There are many examples of full scale testing of bridges (Fletcher and Parker, 2003; Siringoringo and Fujino, 2008; Pakrashi et al., 2013; Sadhu et al. 2015) and a wide range of technologies have been used in such applications (Ko and Ni, 2005). The use of fiber optics has been well established for the monitoring of not only the dynamics of bridges (Salo and Korhonen, 2014; Surre et al., 2013), but also in a structural health monitoring capacity (Scott et al., 2013). The use of non-contact technology has also been investigated, as it offers a more optimized method of testing by removing the need for wiring of the structure, which is labor intensive and economically expensive. In this regard, a number of methods have been proposed and tested, including the use of Geographical Positioning System (GPS) (Meng et al., 2007; Brown et al., 2006; Roberts et al., 2006), Laser Doppler Vibrometer (LDV) (Nassif et al., 2005), image based assessment (Gandhi et al., 2007) and microwave interferometer (Gentile and Bernardini, 2010). Alongside non-contact testing, there is a move in recent times towards the development of wireless sensor

networks which have the advantages of flexibility and value compared to wired systems (Cho et al., 2008; Kurata et al., 2013) and can be coupled with energy harvesting technology to create power independent nodes (Sazonov et al., 2009; Cahill et al., 2013). This removes the need for the replacement of batteries which have finite lifespans, making self-powered wireless sensors an attractive choice for the testing of bridges.

Apart from full scale testing of bridges with new technologies, the modelling of bridge structures has become quite comprehensive investigated as well. Finite element (FE) modelling is popular in the assessment of existing bridges and the updating of such FE models with experimental results is a very effective and powerful tool in this regard (Ren and Peng, 2009; Schlune et al., 2009; Brownjohn and Middleton, 2005). Ambient vibration testing, which does not require excitation equipment, is a very common form of testing (Gentile and Gallino, 2008). Modal testing with excitation equipment is also used, but less so with historic structures. Pedestrian induced results have been used successfully in verifying, refining and updating models. The problem becomes more challenging when information related to a bridge is unknown, uncertain, vague or imprecise and traditional methods of updating or fitting a model by minimizing errors against some benchmark is not an option. Additionally, there is also a need to contribute to the evidence base of full-scale implementation and comparison of different techniques of identifying relevant information about pedestrian bridgtes when a range of instrumentation methods and algorithms are available.

This paper addresses these issues by considering a range of tests and analyses on a historic pedestrian suspension bridge where very little information was available. The as-built geometry was developed as a part of the work due to the absence of any existing drawing and material properties had to be estimated from historic documentation of similar bridges. Effects of damage and variations were partly accounted for by considering a comprehensive inspection fo the bridge. The bridge was tested for static and dynamic responses and these responses were used to update the model to accurately reflect the true behavior of the structure as reasonably as possible. Applications of testing and analysis methods based on video image processing and wavelet packet transformation werevalidated as a part of this experimental campaign. The paper adds to the evidence base of full-scale experimentation of historic pedestrian bridges and compared performance of various analytical and measurement techniques employing different devices in the presence of vague, imprecise and absence of critical information regarding the bridge. The paper illustrated how instrumentation and measurement can aid in developing better numerical models of such bridges in the presence of such uncertainty in information. The performance of different algorithms and measurement methods provide guidance for implementation of different techniques for challenging situations similar to what has been presented.

2 Background Information

Daly's Bridge, built in 1926, is an 87m long steel suspension footbridge spanning River Lee to the west of Cork City, Ireland. It was fabricated by David Rowell & Co. Ltd. London, to the specifications of Cork City Engineer Stephen William Farrington (Irish Arcitectural Archive 2014). As one of only three suspension bridges in Ireland, as well as the only one in Cork, this iconic structure is of great interest and even concern to the public, due to its visible degradation and its dynamic nature (English, 2013; Horgan, 2013).

(a)
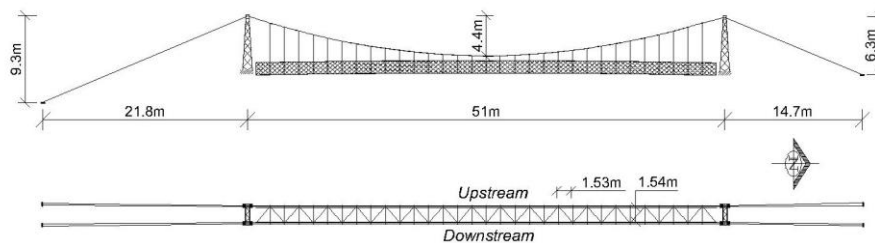
(b)

Figure 1(a). Image and (b). Plan and evelation of Daly's Bridge, Cork City,

Ireland.

The bridge consists of two steel lattice towers, with each tower consisting of
two piers braced together (Figure 1(a)). Saddles mounted on top of the piers
carry four high tension steel cables, with two cables on the upstream side and
two on the downstream side. The cables are anchored to the ground with 8
cast steel sockets in total. The four piers are cast into concrete abutments on
the river banks and the walkway is comprised of vertical steel lattice
parapets. Timber decking and longitudinal diagonal bracing members are
founded on 16 cross beams, which are supported by 32 solid circular steel
hangers. The hangers are suspended from the main cables and connected with
a special Rowell patent clamp which, along with other steel components, was
detailed in a David Rowell patent document and a bill of quantities submitted
to client, Cork City Council.

		Unit
Main Span	50.96	m
Sag	4.131	m
Average Hanger Spacing	1.53	m
Tower Heights	4.222	m
Distance between Main Cables	1.81	m
Distance between Longitudinal Beams	1.48	m
Deck Width	1.45	m
Mass of Deck	157.54	kg/m
Mass of 4 cables per m	29.26	kg/m

Table 1. Geometric data for Daly's Bridge

Key geometrical data was obtained for this study directly from the bridge in
its as-built condition, as summarised in Table 1, as no drawings existed
before this study, with Figure 1(b) showing the as-built drawings. Cross-

sectional details of various sections, such as the main cables, were measured using a vernier callipers and recorded to further increase the accuracy of inputs into the model.

Corrosion was observed to be present in some tower and parapet members, mainly occurring at rigid connection points. The corrosion can be seen in varying stages, owing to partial refurbishment work conducted in the 1980s. The suspension cables are in good condition, showing only surface corrosion along their main span, but minor damage was noted in the free anchor length to the south of the structure, where the highest oscillation amplitudes are observed under pedestrian loading.

3 Initial Finite Element Modelling of Shaky Bridge

The finite element (FE) analysis software Strand 7 (Strand7 Pty Ltd 2014) was used to build a detailed FE model of the structure (Figure 2(a)). The overall geometry of the model reflects the actual shape of the structure and the cross-sectional details match the as-built geometry of each section, measured by the authors for this work using slide calipers, dumpy level and a staff. All members were modelled as beam elements and the suspension cable is modelled using a number of beam elements, similar to other existing works (Xu Y.L and Xia Y, 2012; Kilic et al., 2015; Soyluk et al., 2013). Since the bridge deck is significantly stiff, this approach is deemed adequate for the

scope of the investigation. The connecting clamps between cables and hangers were simplified to beam elements, as shown in Figure 2 (b) .
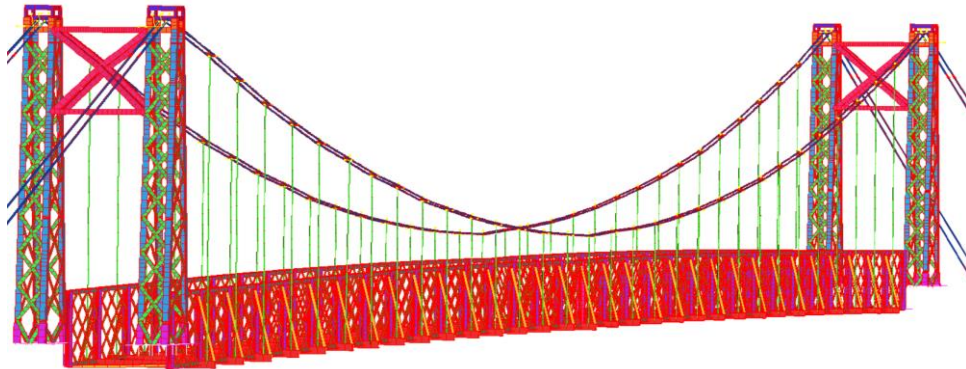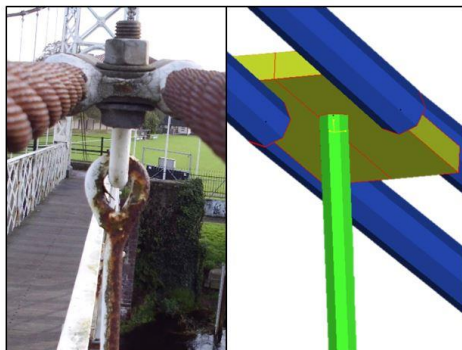

Figure 2 (a) FE model of the bridge
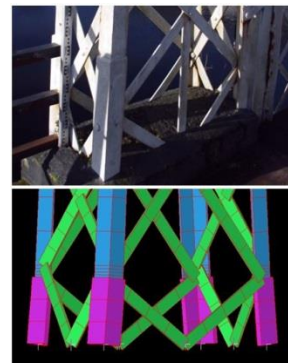

Figure 2(b) Cable hanger connection as-modelled

Figure 2(c) Tower base as-modelled

Member end releases were assigned to represent the as-built condition; the tower bases are cast in concrete and assigned a fully fixed end condition, as

seen in Figure 2(c). Other key connection boundary conditions are summarised in Table 2.

Structural Element	Translation			Rotation		
	X (lateral)	y (longitudinal)	z (vertical)	x	Y	z
Cable Anchor	Fixed	Fixed	Fixed	Free	Free	Free
4 No. Pier Bases	Fixed	Fixed	Fixed	Fixed	Fixed	Fixed
Walkway – Bottom Chord	Fixed	Fixed	Fixed	Free	Free	Free
Walkway – Top chord	Free	Free	Fixed	Free	Free	Free

Table 2. Boundary conditions in FE Model

The material properties were modelled as per specification in the David Rowell patent document. All members are made of steel and a reasonable Young's modulus of 200GPa was set initially. All steel is assumed homogeneous and isotropic. The timber deck was not modelled as the Young's modulus of timber is significantly less than steel.

Initially, the model was validated by visually inspecting the deflected shape and member forces. Numerical validation was then carried out by comparing Strand7 solver results with first principle calculated results (the model used is summarised in Figure 3) where L is the length of the bridge, w is the uniformly distributed load per unit run of the deck, H is the horizontal reaction at the two ends of the cable and V_A and V_B are the vertical reactions at the cable ends.
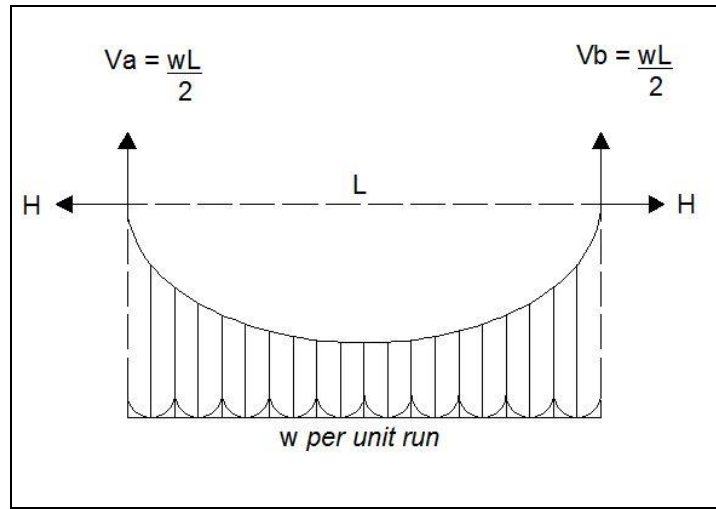
Figure 3. Theoretical cable tension model for a suspension bridge

The theoretical cable tension was calculated as 41.16 kN per cable, compared to 37.34 kN from the FE model. To account for self-weight in the model a tension pre load was applied to the beam members representing the cables and this was calibrated with convergence of mid-span vertical deflection and tower horizontal deflections to 0mm.

4 Static Testing

A static load test under incremental loading was carried out using a Leica NA730 Automatic (optical) level and three 10mm Leica staffs located at both quarter span and at centre span. The bridge was loaded at centre span with an increasing number of people of recorded weights. This was done up to a maximum of 10 people. Staff readings were taken at the unloaded condition and for every increment of two people added to the centre span. A group of 4

people approximately a single point load were then successively placed at a series of positions along the span, and the centre span deflections were measured once the bridge came to rest at each position. From the experimental static tests, an approximation of the influence line diagram was determined, as illustrated by the best fit polynomial of deflection given in Figure 4. The level of accuracy was of the order of 1mm and error bars were of the order of 0.8mm. However, the high magnitude of deflection due to loading can still experimentally be fit to represent a smooth influence line. This was subsequently used successfully as a validation check for the FE model and to approximate the linear and load behaviour of the structure.
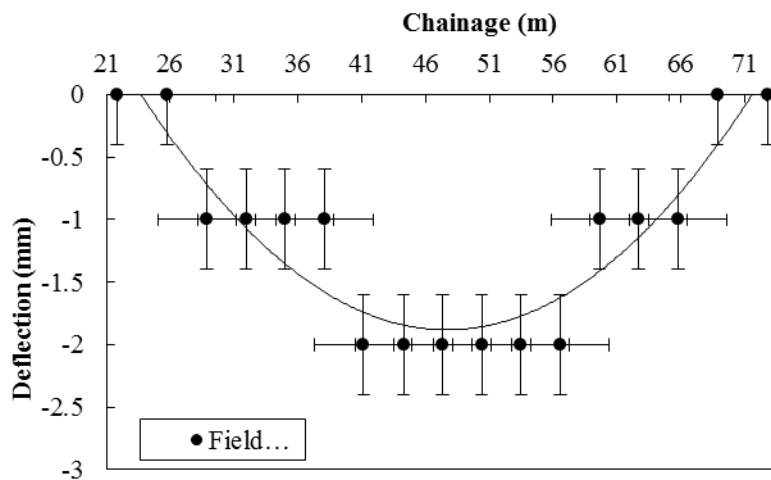
Figure 4. Effect of static loading of pedestrians at various points of bridge.

5 Dynamic Testing

5.1 Instrumentation

In order to determine the dynamic response of the bridge, a wireless sensor network was installed throughout the structure to record the resultant accelerations of the bridge when undergoing various dynamic loading conditions. The individual sensing nodes of this network were developed using ATmega1281 microcontrollers, LIS3331LDH STMicroelectronics accelerometers and an XBee-ZB-PRO ZigBee module for networking. The LIS3331LDH is a tri-axial, 16-bit acceleration sensor which has a range of $\pm 2g$ and was sampled at 50Hz. The acceleration noise density was 218 $(\mu g)/\sqrt{Hz}$, resulting in a root mean squared (RMS) acceleration noise of 1.93mg. The nodes were arranged in a star topology (Buratti et al., 2009) and measurements were initialized by a co-ordinator at the topological centre of the network. The time and acceleration data was recorded and stored locally on an SD card connected to each node. A total of eight nodes were utilised and applied at locations along the deck and cables of the bridge (Figure 5(a)), with the nodes along the deck being held in place using a mounting bracket which was fixed to the bridge (Figure 5(b)). For the attachment to the cables, a clamp was designed so as to connect the two cables via a platform on which the sensor could be affixed (Figure 5(c)) and a SolidWorks 3D model of this allowed the clamp to be constructued using 3D printing technology. Such design ensured full contact between sensor and the two cables of the super structure.
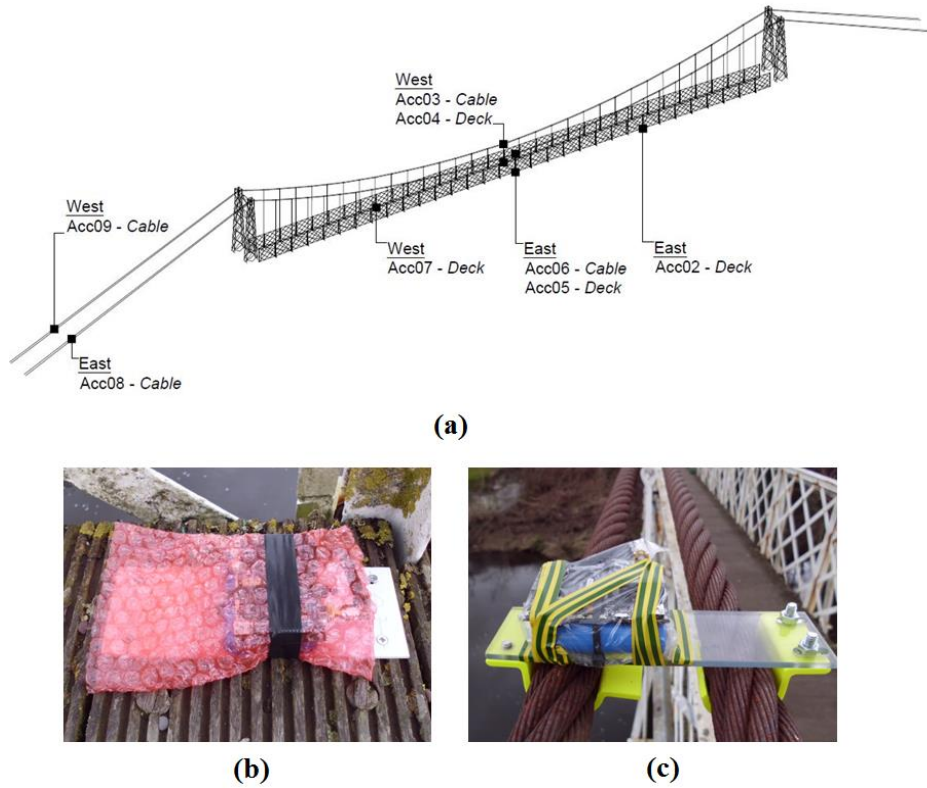
Figure 5 (a) Sensor locations (b) Sensor attachment to deck and (c) Sensor attachment to cables

Data was continuously recorded on the accelerometers for the bridge at rest, for controlled pedestrian and cyclist tests for periods of approximately 90 seconds and 75 seconds respectively, including settling periods before and after, during which no other excitation source was present, and for all members of the public who passed during this period.

5.2 Video Based Tracking

A video based tracking capable of analysing bridge vibrations characterised by large amplitudes and low frequencies, was employed to obtain further information about the bridge from an alternative technology application as a

test case. The video analysis operates by tracking the movement of points on the bridge whilst in an excited state. Several points at the mid-span of the bridge, as indicated in Figure 6 (a), were captured by a video camera that was positioned on the bank of the river, as shown in Figure 6 (b). The pixel locations for these tracked points were identifed in each frame over the course of the video, which resulted in a time series corresponding to the dynamic displacement responses of the bridge. Spectral analysis could then to be performed on the signal in order to identify the major frequency components. By tracking 3 distinct points (Figure 6) stereoscopically on the bridge as recorded on video at a rate of 35 frames per second (FPS), their movement in the vertical plane in terms of pixels and sub-pixels was monitored from frame to frame.

Figure 6 (a) Tracked points at the centre of the span used in video based analysis, and (b) Position of the video camera in relation to the bridge.

5.3 iPhone application

An iPhone was attached to the handrail of the bridge and a commercial application was used to obtain an estimate of the bridge's natural frequency in order to see if 'off-the-shelf', cheap instrumentation can estimate the dynamical response of the bridge, and to what extent. The 'off-the-shelf'

15

application may be a cheap yet effective tool in certain cases, and its reliability might be worth investigating. 'Vibration' version 2.0 is a smartphone application which uses the internal accelerometer and gyroscope of the device to analyse vibratory and rotational motion, and it was used to obtain an estimate of the natural frequency of the bridge.

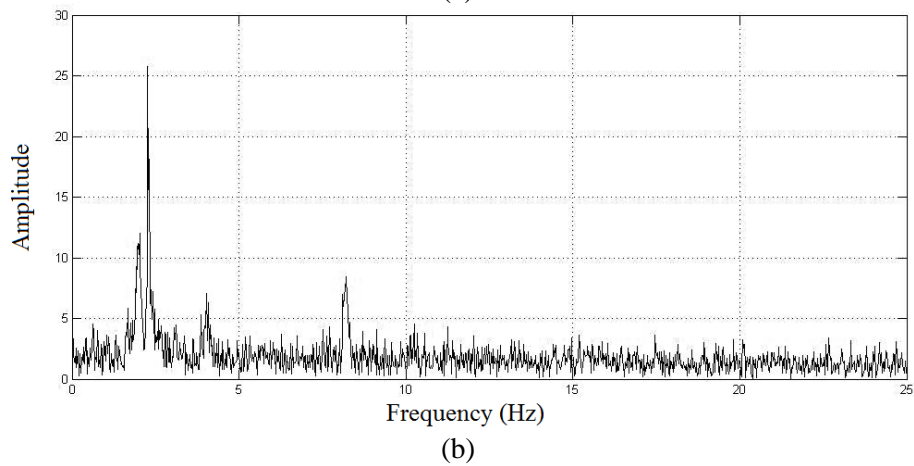## 6 Analysis of Dynamic Experimental Data

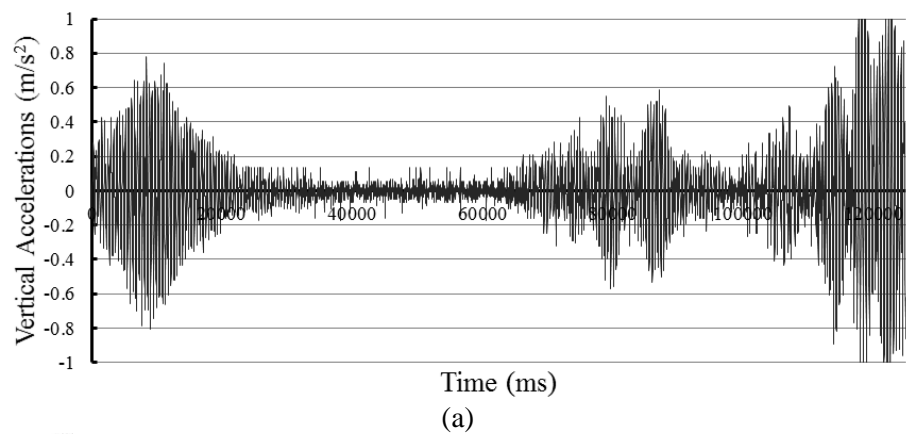### 6.2 Acceleration Data

(a)

(b)

Figure 7. Typical data controlled walking test with (a) Accelerations (b)

Frequency spectrum plot

For the three types of dynamic testing of the bridge structure, the acceleration was initially recorded in a 64 bit format and subsequently converted into SI units. From this, the response of the bridge in the frequency domain was obtained through a Fast Fourier transform (FFT). Figure 7 illustrates typical acceleration and corresponding frequncey profiles obtained from the testing and subsequent analysis.

The results from different runs of the same controlled test show good repeatability in the experiments, with the RMS values for accelerations of different experiments deviating by no more than 5%. Results aligned to what was observed in field observations- little response was observed for the cyclist and highest response observed and recorded was for groups of pedestrians. The average RMS accelerations at mid-span, presented in Table 3, should be read with the context of serviceability limit on the peak value of such accelerations as 0.7 m/s^2 as per EN 1990 A2.4.3.2(1).

Load Condition	Average RMS Acceleration at Mid-span
Rest	0.036 m/s^2
Cyclist	0.048 m/s^2
RW* Walking	0.11 m/s^2
DOD* Walking	0.38 m/s^2
Pair Pedestrians	0.49 m/s^2

Group of Pedestrians	0.51 m/s^2

Table 3. Summary of RMS acceleration values

The natural frequency was found by peak-picking using acceleration data for the ambient vibration of the bridge.

6.2 Video Based Testing Data

To analyse the data from the video based testing, in each successive frame, several distinctive points (e.g. high-contrast corrosion spots that could be uniquely identified) were chosen to be tracked. Picking multiple points in this manner enabled more robust and effective tracking from frame to frame. Tracking is done by picking a small sliding window, *SW*, which is centred on the chosen point in the first frame of a video sequence and following it throughout the duration of the video clip. For every successive frame, the point is located by finding the patch which best correlates with the patch in the previous frame. The best correlation was determined using the Zero-mean Normalised Cross Correlation (ZNCC) metric. For this task, the ZNCC is defined as:

$$\psi = \frac{\sum\limits_{u,z \in SW} (\Gamma_{\ell+1}(u,z)_{ab} - \overline{\Gamma}_{\ell+1,ab})(\Gamma_{\ell}(u,z) - \overline{\Gamma}_{\ell})}{\sqrt{\sum\limits_{u,z \in SW} (\Gamma_{\ell+1}(u,z)_{ab} - \overline{\Gamma}_{\ell+1,ab})^2 (\Gamma_{\ell}(u,z) - \overline{\Gamma}_{\ell})^2}} \quad a,b \in SS \quad \text{(Eq. 1)}$$

where $f_n(u,z)$ and $f_{n+1}(u,z)$ denote the intensity values in the window, *SW*, centred on the point being tracked in the nth and $n+1^{th}$ frame respectively , *u* and *z* are the horizontal and vertical spatial indices of the of *SW*, *a* and *b* are the horizontal and vertical indices of the stationary region *SS*, and $\overline{\Gamma}_n$ and $\overline{\Gamma}_{n+1}$ are the mean pixel intensity values within the area of the *SW* for the nth frame, and within *SS* for the $n+1^{th}$ frame. The pixel locations for the tracked point are recorded at each frame are used to create a plot of time versus displacement from the video footage. A detailed account of the methodology has been reported by O'Byrne et al. (2015).

A Fourier transform of the obtained signal could then identify natural frequency as described before and this estimate was found to correlate well with the other methods, as shown in Table 4. It is interesting to note the relatively good performance of the iPhone application. These results encourage more detailed assessment of various off-the-shelf cheap products for different applications to identify their limits of applicability. The authors note that such off –the-shelf product can be helpful when lower freuqncies, typically less than 5Hz, are of interest but detailed investigation into different phones and applications are required to quantify their performance for a range of frequencies before conclusive recommendations around the use of smartphones can be developed.

	Mean Natural Frequency	Standard Deviation from Mean, %
Accelerometers	2.265 Hz	4.41

Phone Application	2.17 Hz	-
Image method	2.11 Hz	1.56

Table 4 Sensor fusion comparison

7 Modal Identification using Wavelet Packet Transform

7.1 Wavelet Packet Tranformation-based output-only modal indentfication

The modal parameters of the bridge from the vibration data was estimated using a newly established wavelet-based signal processing method (Sadhu 2013) to test its effectiveness. A brief overview of the method is outlined below followed by the application of this method using the pedestrian-induced vibration of the Shaky bridge. For the details of this method, the readers are directed to some recent publications (Sadhu 2013; Sadhu et al. 2014). A short account of the method is presented here for completeness. Consider a linear, lumped-mass and classically damped dynamical system with n_d degrees-of-freedom (DOF), subjected to an excitation force, F(t).

$$M\ddot{x}(t) + C\dot{x}(t) + Kx(t) = F(t)$$ (Eq. 2)

where, x(t) is a vector of displacements at DOFs. M, C, and K are the mass, damping and stiffness matrices of the multi-degree-of-freedom (MDOF) system respectively. The measured signal at the ith channel of sensor of Equation 2 can be expressed as

$$x_i(t) = \sum_{l=1}^{n_x} A_{il} s_l(t) \quad i = 1, 2, ..., n_m$$ (Eq. 3)

Considering the wavelet packet transformation (WPT) of the sensor responses and the sources at any specific node (j; v) (see Appendix for details), and applying the ortogonallity condition at highest scale level for a selected wavelet basis function, Equation 3 yields (Sadhu et al. 2011):

$$f_{k,i}^{s,v}(t) = A_{il} e_{k,l}^{e,v}(t) \qquad \text{(Eq. 4)}$$

This equation relates the WPT coefficient of the ith channel measurements with the WPT coefficients of the lth modal response. Therefore, following the same logic for two sensor measurements, say $i = q$ and $i = r$, the partial mixing matrix coefficients of the qth sensor measurement normalized with respect to the rth measurement are obtained as

$$\frac{f_{k,q}^{s,v}}{f_{k,r}^{s,v}} = \frac{A_{ql} e_{k,l}^{s,v}(t)}{A_{rl} e_{k,l}^{s,v}(t)} = \frac{A_{ql}}{A_{rl}} = \widehat{a_{ql}}; \qquad l = 1, 2, \ldots n_s \qquad \text{(Eq. 5)}$$

Then, $\widehat{a_{ql}} = \dfrac{A_{ql}}{A_{rl}}$ represents the estimated normalized mixing matrix coefficient of the lth mode at the qth DOF. Therefore, the normalized partial mixing matrix coefficients can be readily estimated using the WPT coefficients of the sensor measurements.

7.2 Modal Identification of Shaky Bridge under Pedestrian Walking

When a light-weight and flexible pedestrian bridge like Daly's bridge is excited by a pedestrian walking with low excitation frequencies (say 1.5-2.5 Hz), identication of inherent structural frequencies can be difficult. Since the pedestrian excitation lies within the range of natural freuqencies of the

bridge, the main challenge here is to distinguish between the natural frequency and the pedestrian excitation frequency. Figure 8 shows the Fourier spectra of such a pedestrian-induced vibration data at the middle of the span of the bridge. When the pedestrian (i.e. RW) walks at a frequency of 1.7 Hz (measured by metronome), there is a significant energy in addition to the structural frequency (i.e. 2.2 Hz). On the other hand, resonance occurs when the walking frequency coincides with the structural frequency in case of second pedestrian (i.e. DOD). Therefore it is clear that distinguishing structural frequencies from excitation frequency from output-only vibration data (without having any information about excitation) is a challenge. In this regard, wavelet packet decomposition as outlined above is employed for system identication.
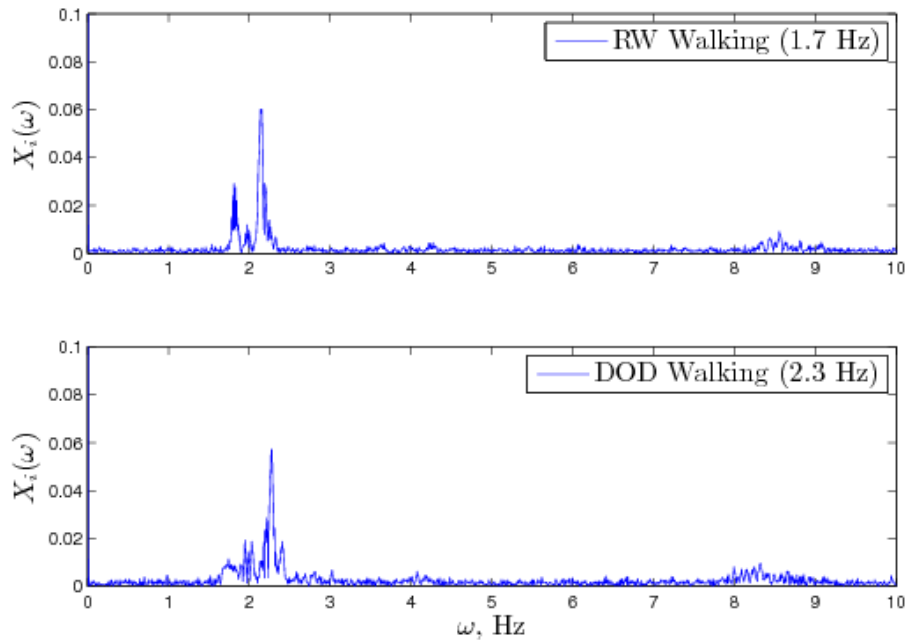
Figure 8 Fourier spectra of vibration data under various pedestrians walking

The vibration data under RW walking is utilised. First, the acceleration at the mid-span of the bridge is decomposed using wavelet packet transform (WPT). Depending on the sampling frequency (i.e., 50 Hz) and lower frequency of interest, a scale level (s) of 6 is chosen for the WPT. The wavelet basis is selected as *db5*, an orthogonal basis that is suitable for oscillating vibration data. WPT of vibration data results in various low and high frequency coefficients (Mallat, 1998) that are mono-component (i.e. single frequency) in nature. Since $s = 6$, a total number of $2^6 = 64$ coefficients are generated.
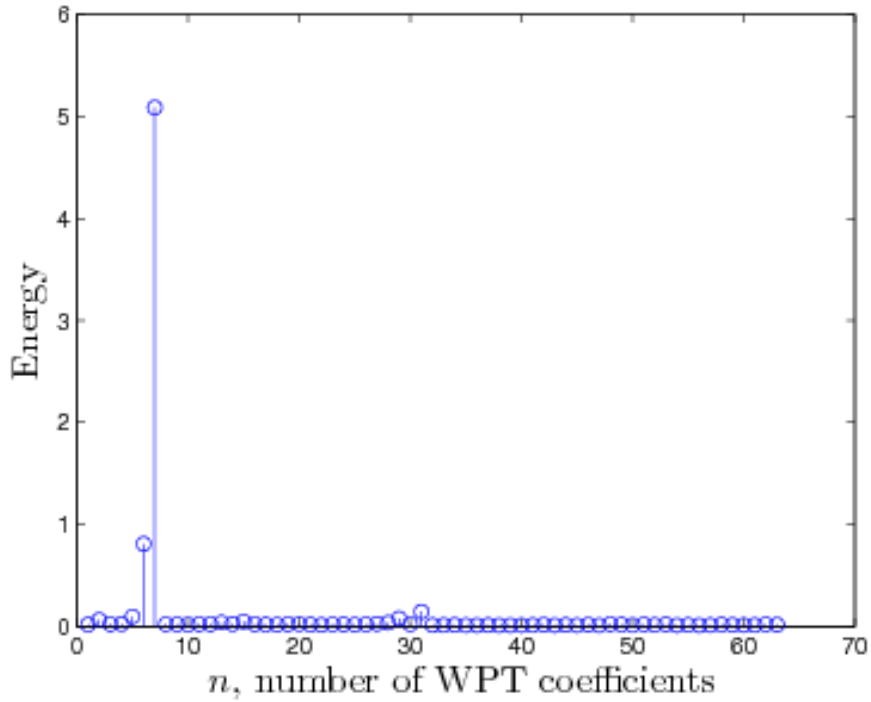
Figure 9 Energy of various WPT coefficients

Figure 9 shows the energy of each of these coefficients and reveals that only two coefficients (i.e., $n = 6$ and $n = 7$) contain significantly higher energy compared to other 62 coefficients. Such a diagram can be used to identify potential WPT coefficients with significant dynamical information (Sadhu 2013). In fact, these two coefficients comprise of dominant frequencies that are present in the data. In this way, key frequency components (either structural or excitation) are extracted from acceleration data in adaptive way as shown in Figure 10.
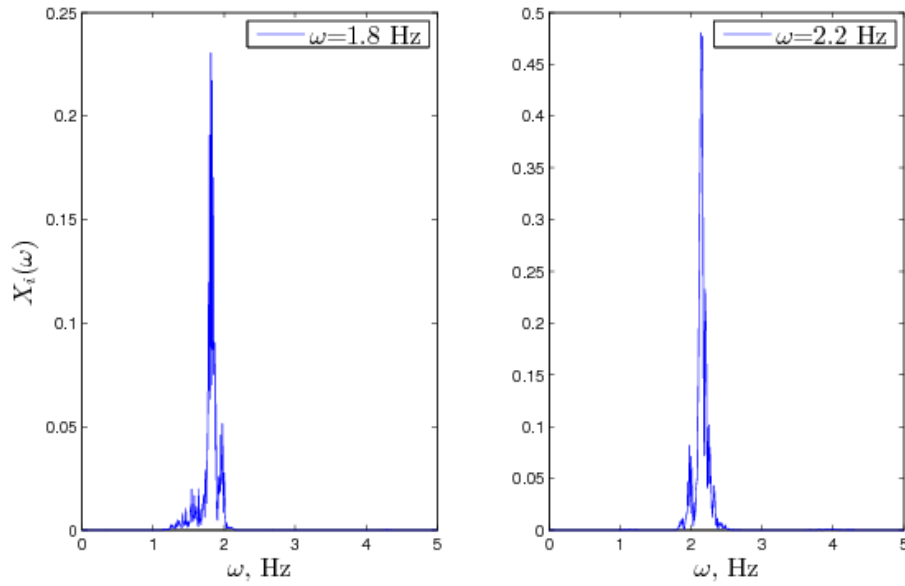
Figure 10 Fourier spectra of selected WPT coefficients (n = 6; 7) with higher energy content

Figure 11 shows the time-history of these two WPT coefficients. It reveals that the WPT coefficient with $\omega = 1.8$ Hz has a nice deterministic envelope from which it can be adopted as pedestrian-walking frequency component

(the exact value is 1.7 Hz). On the other hand, $f_a^{6,7}$ has a random envelope contributing to the structural frequency. In this way, structural and excitation frequencies are separated. Similar analysis is performed using the vibration data of the sensor installed at quarter span of the bridge. Once the modal response is identified, the auto-correlation function (ACF) is developed and the damping of the first vertical mode is estimated as 0.31% using the exponential fitting of ACF (Magalhã̃es et al., 2010) as shown in Fig. 12. However, this estimate can and will vary based on the type of responses obtained and the methodology followed and a variation around estimates of low damping ratios are generally expected.
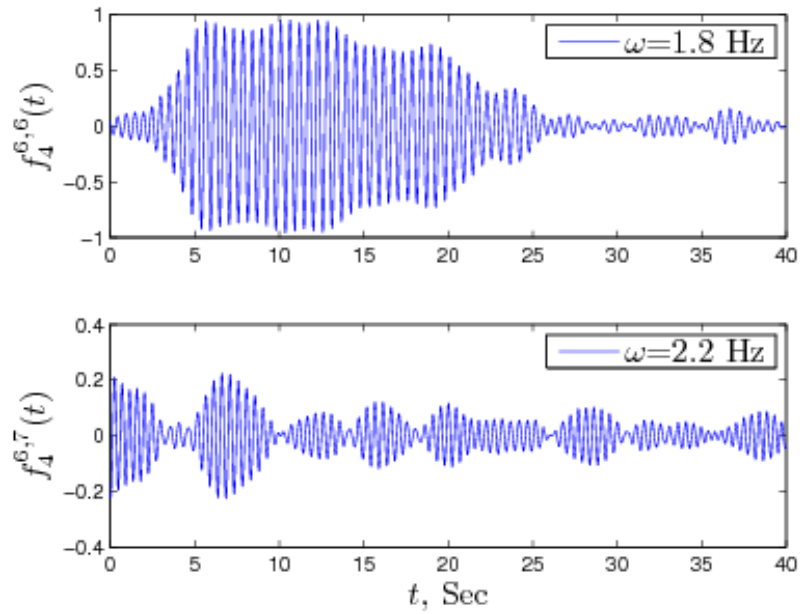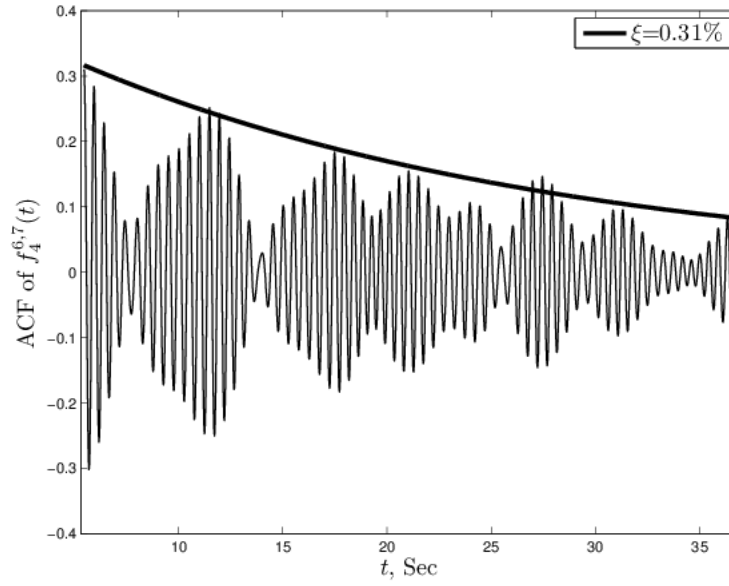

Figure 11. Key WPT coefficients

Figure 12: Estimation of damping for the first vertical modal response

Apart from the vertical response, the above analysis is repeated in the lateral response of the bridge collected using the tri-axial sensors. Figure 13 shows the modal response and FFT of first lateral (i.e., 1.1 Hz) and torsional mode (i.e., 3 Hz) identified using the WPT method. The type of torsional mode is identified based on its presence in both vertical and lateral measurements. It may be observed that there is a slight energy contribution of the torsional mode around 3 Hz in Figure 8. A detailed comparison of the FE and identified modal freuqnecies, approximated to the first digit after the decimal point, is listed in Table 5.

Modes #	FE (Hz)	Identified (Hz)
1	1	1.1
2	2	2.2
3	3	3.0

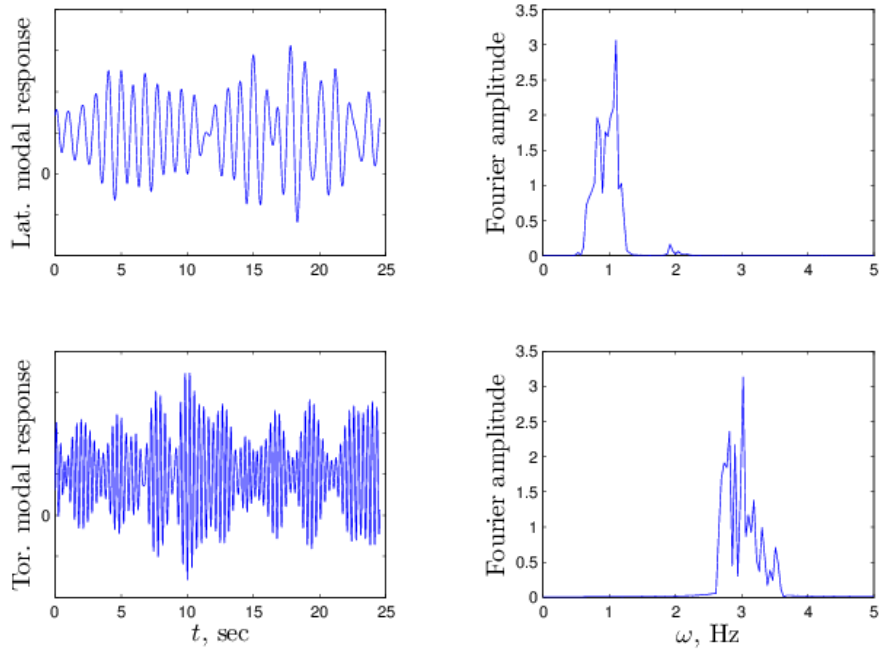Table 5: Comparison of exact and identified modal frequencies

Figure 13: Identified lateral and torsional modal responses

8 Finite Element Model Updating Incorporating Experimental Analysis

The method of static testing in the field in the form of incremental point loading at centre span, was replicated in the FE model in order to compare field and model deflection results. An influence diagram for a moving point load was also generated. The first vertical mode shape of the model, which corresponds to the natural frequency of the bridge, was identified using the programs natural frequency solver (Figure 14).
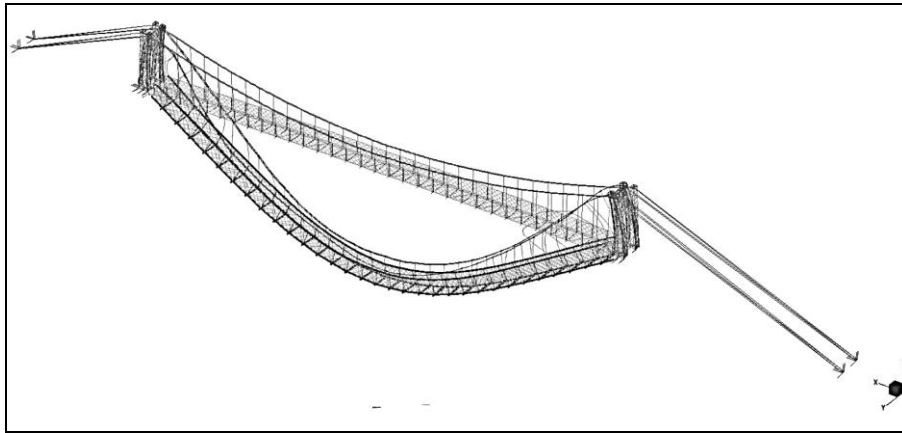
Figure 14 First vertical modeshape

8.1 Model Modifications

A series of adjustments were made to the original model, based on physical observations of the structure, with the intention of improving the accuracy of model outputs with reference to the field results.

Model Number	Description
1	Original model (E = 200GPa)
2	Subdivision of elements
3	Change of cable diameter
4	Damaged model
5	Change of Young's Modulus (E = 195GPa)

Table 6 Model Revisions

A summary of the model revisions is shown in Table 6. A refined model with subdivided elements was created to improve accuracy of the behaviour of the model (Model 2). A further modification was made by reducing the cross-sectional area of the cables (Model 3), to account for the true effective cross-sectional area due to the stranded nature of the cables. A damaged model was generated by removing members identified in a field survey as structurally deficient (Model 4). And finally, a model of reduced Young's modulus was

created to account for less standardised production when the members were created almost 90 years ago (Model 5).

8.2 Comparison of Results

Static and dynamic properties were monitored and recorded for each iteration of the model, resulting in gradually improved accuracy of the model's behaviour (Figure 15).
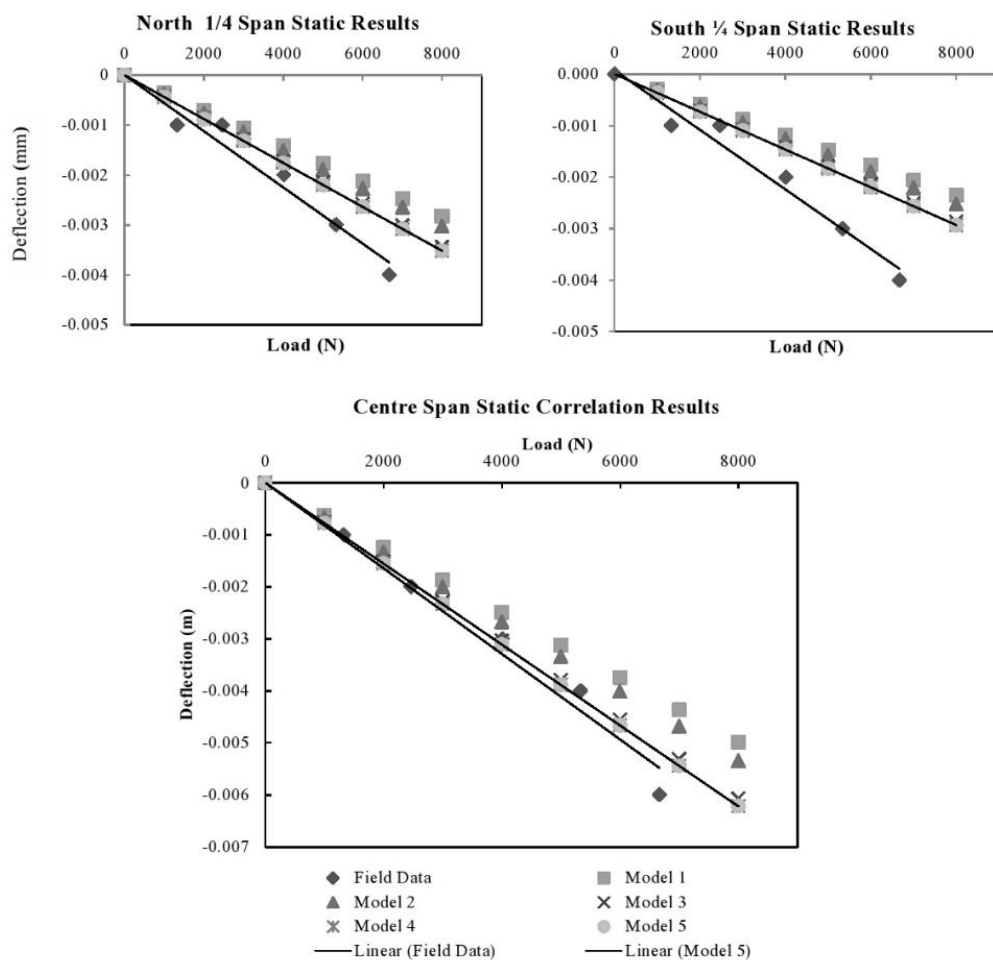

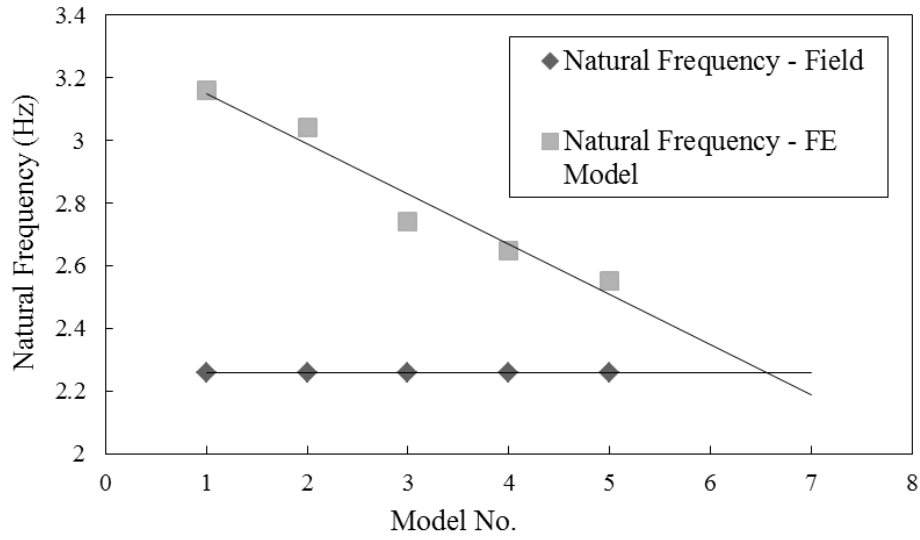Figure 15. Static Deflection comparison

Figure 16. Converge of Natural Frequency of Model to Field Results

There is a continually improved degree of convergence, as shown in Figure 16, from model 1 to model 5 when comparing the natural frequency between field results and model results. A number of iterative schemes for ideal situations are not applicable here dur to the number of the unknown factors affecting the real behavious of the model and the uncertainty or lack of information around them. Nevertheless, practical considerations, along with modelling and experimentation leads to a natural frequency of 3.16Hz for Model 1, 3.041Hz, 2.742Hz and 2.649Hz for Models 2, 3 and 4 respectively, until the final model (Model 5) reaches a natural frequency of 2.553Hz. With each model, the accuracy of both the natural frequency and the mid-span deflection of the model increased in accuracy compared with the experiemental results. This is illustrated in Table 7, whereby the percentage values representing the deviation from the field data of the model's value

improves, up to a final 87.8% accuracy in natural frequency for Model 5 and a corresponding 3.2% accuracy in the mid-span deflection. While the stiffness of the bridge in the model can be artificially changed to match the mid-span deflection and corresponding natural frequency can be computed, this would not be based on physical evidences or reasons as has been considered for other models. Under such circumstances, Model 5 is the best performance available considering explanations related to the realistic condition of the bridge and the remaining convergence can be attributed to a combination of unknown information, which were not identified in this study.

Model No.	Natural Frequency %	Middle span Deflection %
Model 1	33.2	43.9
Model 2	29.5	32.7
Model 3	19.3	10.1
Model 4	15.9	5.6
Model 5	12.2	-3.2

Table 7. Deviation from field results in improved models

9 Discussions and Conclusions

An experimental and theoretical study on an iconic steel suspension footbridge in Cork is represented in this paper. An Finite Element (FE) model was created based on a geometric field survey and historic documentation on the components and material of the structure. The bridge was instrumented at multiple locations using sensors, and a novel video imaging system and

iPhone application were also employed to obtain dynamic and modal information about the structure. Static responses to the bridge were obtained using a dumpy level. Results from these methods were used to fine tune the FE model so that it reflected, with reasonable accuracy, the behavior of the bridge. The bridge exhibits strong dynamic behavior due to its natural frequency being similar to the frequency of the walkers. The corrosion of elements is shown, via the damaged model, to have a significant effect on the global behavior of the structure. This work shows how careful modelling can improve estimates and be helpful in difficult situations where drawings, material properties and boundary conditions may not be available, where otherwise an estimate may be impossible to obtain. The correlation of different sensors shows a benefit to the fusion of technologies and the relative merits of different systems. In this paper, wavelet packet decomposition based method has been adopted to separate structural and excitation frequencies from the output-only vibration data. In the absence of any information of excitation, such an approach will be also be effective in estimating structural frequency and damping that might be useful in controlling the vibration performance of the bridge including designing of passive and semi-active control devices like tuned-mass dampers.

References

American Society of Civil Engineers, 2013. www.infrastructurereportcard.com. Available at: http://www.infrastructurereportcard.org/a/#p/bridges/overview [Accessed November 12, 2014].

Brown C, Roberts G and Meng X (2006) Developments in the use of GPS for bridge monitoring. Proceedings of the Institution of Civil Engineers – Bridge Engineering 159(3): 117–119.

Brownjohn JMW and Middleton C (2005) Efficient dynamic performance assessment of a footbridge. Proceedings of the Institution of Civil Engineers – Bridge Engineering 158(4), 185–192.

Bruno L and Venuti F (2009) Crowd–structure interaction in footbridges: Modelling, application to a real case-study and sensitivity analyses. Journal of Sound and Vibration 323(1-2) 475–493.

Buratti C, Conti A, Dardari D and Verdone R (2009) An overview on wireless sensor networks technology and evolution. Sensors 9(9) 6869–96.

Caetano E, Barbosa R, Cunha Á and Magalhães F (2013) The Viana footbridge: construction and dynamic monitoring. Proceedings of the Institution of Civil Engineers – Bridge Engineering 166(4), 273–290.

Cahill P, Nuallain NAN, Jackson N, Mathewson A, Karoumi R and Pakrashi V (2014) Journal of Bridge Engineering ASCE 19(9) 04014043.

Catbas FN, Susoy M, and Frangopol DM (2008) Structural health monitoring and reliability estimation: Long span truss bridge application with environmental monitoring data. Engineering Structures 30(9) 2347 – 2359.

Cho S, Y CB, Lynch JP, Zimmerman A, Spencer B, Nagayama T (2008) Smart wireless sensor technology for structural health monitoring of civil structures. International Journal of Steel Structures 8(4) 267-275.

English E (2013) 'Iconic Shaky Bridge in need of some TLC' Irish Examiner. See http://www.irishexaminer.com/ireland/iconic-shaky-bridge-in-need-of-some-tlc-236389.html [Accessed 01/07/ 2016]

Fletcher MS and Parker JS (2003) Dynamics of the Hungerford Millennium footbridges, UK. Proceedings of the Institution of Civil Engineers – Bridge Engineering 156(2), 57–62.

Gandhi T, Chang R and Trivedi MM (2007) Video and seismic sensor based structural health monitoring: framework, algorithms, and implementation. IEEE Transactions on Intelligent Transportation Systems 8(2) 169-180.

Gentile C and Bernardini G (2010) An interferometric radar for non-contact measurement of deflections on civil engineering structures: laboratory and full-scale tests. Structure and Infrastructure Engineering 6(10), 521–534.

Gentile C and Gallino N (2008) Ambient vibration testing and structural evaluation of an historic suspension footbridge. Advances in Engineering Software 39(4) 356–366.

Horgan P (2013) 'Shakey times for dalys bridge'. Cork Independent. See http://www.corkindependent.com/20130711/news/shakey-times-for-dalys-bridge-S68737.html [Accessed 01/07/2016]

Huang H, Thambiratnam DP and Perera NJ (2005) Resonant vibration of shallow suspension footbridges. Proceedings of the Institution of Civil Engineers Engineers – Bridge Engineering 158(4), 201–209.

Ingólfsson ET, Georgakis CT and Jönsson J (2012) Pedestrian-induced lateral vibrations of footbridges: A literature review. Engineering Structures 45 21–52.

Irish Architectural Archive (2014) Dictionary of Irish Architects. See http://www.dia.ie/architects/view/1862/farrington-stephenwilliam#tab_works [Accessed 01/07/ 2016].

Jaksic V, O'Connor A and Pakrashi V. (2014). Damage Detection and Calibration from Beam-Moving Oscillator Interaction Employing Surface Roughness. Journal of Sound and Vibration 333(17) 3917-3930.

Jaksic V, Mandic DP, Karoumi R, Basu B and Pakrashi V.(2016) Estimation of nonlinearities from pseudodynamic and dynamic responses of bridge structures using the Delay Vector Variance method. Physica A: Statistical Mehcanics and its Applications, 441, 100-120.

Kilic SA, Raatschen HJ, Körfgen B, Astaneh-Asl A and Apaydin NM. (2015). Proceedings of the International Conference on Multi-Span Large Bridges, Porto, Potugal.

Ko JM and Ni YQ (2005) Technology developments in structural health monitoring of large-scale bridges. Engineering Structures 27(12)1715–1725.

Kurata M, Kim J, Lynch, J, Van Der Linden, GW, Seddat H, Thometz E, Hipley P and Sheng LH (2013) Internet-enabled wireless structural monitoring systems:development and permanent deployment at the new carquinez suspension bridge, Journal of Structural Engineering ASCE 139(10) 1688 – 1702.

Leonard D (1966) Human tolerance levels for bridge vibrations. Crowthorne.

Magalha˜es F, Cunha A, Caetano E and Brincker R. (2010). Damping estimation using free decays and ambient vibration tests. Mechanical Systems and Signal Processing, 24, 1274-1290.

Mallat SG (1998) A wavelet tour of signal processing. Academic Press, San Diego.

Meng X, Dodson AH and Roberts GW (2007) Detecting bridge dynamics with GPS and triaxial accelerometers. Engineering Structures 29(11) 3178–3184.

Nakamura S and Kawasaki T (2006) Lateral vibration of footbridges by synchronous walking. Journal of Constructional Steel Research 62(11) 1148–1160.

Nassif HH, Gindy M and Davis J (2005) Comparison of laser Doppler vibrometer with contact sensors for monitoring bridge deflection and vibration. NDT & E International 38(3) 213 – 218.

O'Byrne M, Ghosh B, Schoefs F, O'Donnell D, Wright W and Pakrashi V. (2015). Acquisition and Analysis of Dynamic Responses of a Historic Pedestrian Bridge using Video Image Processing. Institute of Physics Journal of Physics 628 012054-1-8.

Pakrashi V, Harkin J, Kelly J, Farrell A and Nanukuttan S (2013) Monitoring and Repair of an Impact Damaged Prestressed Concrete Bridge. Proceedings of the Institute of Civil Engineers - Journal of Bridge Engineering 166(1) 16-29.

Pakrashi V, O' Connor A and Basu B (2010) A Bridge – Vehicle Interaction Based Experimental Investigation of Damage Evolution. Structural Health Monitoring 9(4) 285-296.

Ren WX and PengXL (2005) Baseline finite element modeling of a large span cable-stayed bridge through field ambient vibration tests. Computers & Structures 83(8-9) 536–550.

Roberts G, Meng X, Brown C and Dallard P (2006) GPS measurements on the London Millennium Bridge. Proceedings of the Institution of Civil Engineers – Bridge Engineering 159(4), 153–161.

Sadhu A, Hazra B, Narasimhan S and Pandey MD (2011) Decentralized modalidentification using sparse blind source separation. Smart Materials and Structures 20(12) 125009.

Sadhu A (2013) Decentralized ambient modal identification of structures. PhD Thesis, Department of Civil and Environmental Engineering, University of Waterloo, Canada.

Sadhu A, Narasimhan S and Goldack A (2014) Decentralized modal identification of a pony truss pedestrian bridge using wireless sensors. Journal of Bridge Engineering ASCE 19(6) 04014013.

Sadhu A, Narasimhan S and Goldack A (2015) Ambient modal identification using multi-rank parallel factor decomposition. Structural Control and Health Monitoring 22(4) 595 – 614.

Salo J and Korhonen I (2014) Calculated estimate of FBG sensor's suitability for beam vibration and strain measuring. Measurement 47 178–183.

Sazonov E, Li H, Curry D and Pillay P (2009) Self-Powered Sensors for Monitoring of Highway Bridges. IEEE Sensors Journal 9(11) 1422 – 1429.

Schlune H, Plos M and Gylltoft K (2009) Improved bridge evaluation through finite element model updating using static and dynamic measurements Engineering Structures 31(7) 1477 – 1485.

Scott RH, Banerji P, Chikermane S, Srinivasan S, Muhammed Basheer PA, Surre F, Sun T and Grattan KTV (2013) Commissioning and evaluation of a fiber-optic sensor system for bridge monitoring. IEEE Sensors Journal (13)7 2555-2562.

Siringoringo DM and Fujino Y (2008) System identification of suspension bridge from ambient vibration response. Engineering Structures 30(2) 462 – 477.

Soyluk K, Kartel H and Adanur S. (2013). Comparison of Dynamic Behaviour of Long-Span Cable-Supported Bridges. Vienna Congress on Recent Advances in Earthquake Engineering and Structural Dynamics 2013 (VEESD 2013), Vienna, Austria.

Strand7 2.4.4 (2014) [Computer software] Sydney, New South Wales, Australia, Strand 7 Pty.

Surre F, Sun T and Grattan KT (2013) Fiber optic strain monitoring for long-term evaluation of a concrete footbridge under extended test conditions. IEEE Sensors Journal 13(3) 1036 – 1043.

Van Nimmen K, Lonbaert G, de Roeck G and Ven den Broeck P (2014) Vibration serviceability of footbridges: Evaluation of the current codes of practice. Engineering Structures 59 448–461.

Wickerhauser M (1994) Adapted Wavelet Analysis from Theory to Software. A. K. Peters Ltd., Wellesley, Massachusetts.

Xu Y.L and Xia Y (2012) Structural Health Monitoring of Long Span Suspension Bridges. CRC Press, Taylor and Francis Group, Boca Raton, Florids, USA.

Živanović S, Pavic A and Reynolds P (2005) Vibration serviceability of footbridges under human-induced excitation: a literature review. Journal of Sound & Vibration 279(1-2) 1-74.

Živanović S, Pavic A and Reynolds P (2006) Modal testing and FE model tuning of a lively footbridge structure. Engineering Structures 28(6) 857–868.

Znidaric A, Pakrashi V, O' Connor A and O' Brien E (2011) A Review of Road Structure Data in Six European Countries. Proceedings of the Institution of Civil Engineers - Journal of Urban Design and Planning 164(4), 225-232.

APPENDIX

Wavelet Packet Transform (WPT)

WPT offers a complete level-by-level decomposition, where both the details as well as the approximations are decomposed in a sequential digital altering process (Wicker-hauser 1994). The WT of a signal y(t) is its orthogonal decomposition of the form (Mallat 1998):

$$d_k^j(y) \triangleq \left\langle y(t) \left| 2^{-j/2} \psi^* \left(\frac{t-k}{2^j} \right) \right. \right\rangle = \frac{1}{2^{j/2}} \int_{-\infty}^{\infty} y(t) \psi^* \left(\frac{t-k}{2^j} \right) dt.$$

where the function ψ is commonly known as the mother wavelet and * stands for complex conjugation. The indices j and k denote the scale and translation parameters, respectively. The transformation is computed at discrete values on a grid corresponding to dyadic values of scales (2^j) and translations (k), where k; j $\in Z^2$ i.e., integers. The original signal $y(t)$ can be expressed in terms of wavelet coefficients d_k^j as:

$$y(t) = \sum_j \sum_k d_k^j \psi_k^j(t)$$

WPT is an extension of the WT and can be implemented by a generalization of the pyramidal algorithm. A wavelet packet is a triple-index function

$\psi_k^{j,v}(t)$, where v can beinterpreted as frequency parameter, and a WPT basis

is defined as (Sadhu 2013):

$$\psi_k^{j,v}(t) = \frac{1}{2^j} \psi^v(\frac{t-k}{2^j})$$

where,   please insert phi(t) and psi(t) represent the scaling and wavelet

functions, respectively. The wavelet packet coefficients at each node (*j, v*) are

written as:

$$w_k^{j,v}(y) \triangleq \left\langle y(t) \Big| 2^{-j/2} \psi^v\left(\frac{t-k}{2^j}\right) \right\rangle = \frac{1}{2^{j/2}} \int_{-\infty}^{\infty} y(t) \psi^v\left(\frac{t-k}{2^j}\right) dt.$$

The original signal y(t) can be written as a summation of all the wavelet

packet component signals, $y^{j,v}$ (Sadhu 2013):

$$y(t) = \sum_{v=0}^{2^j-1} y^{j,v} = \sum_{v=0}^{2^j-1} \sum_k w_k^{j,v} \psi_k^{j,v}(t)$$

The above expression represents complete wavelet packet decomposition of a

vibration signal and is exploited in the above WPT-based modal

identification method.

List of Figures

Table 1 Geometric data for Daly's Bridge

Table 2 Boundary conditions in FE Model

Table 3 Summary of RMS acceleration values

Table 4 Sensor fusion comparison

Table 5 Comparison of exact and identified modal frequencies

Table 6 Model Revisions

Table 7 Accuracy of field results to improved models